EFFECTS OF WAVE, TIDAL CURRENT AND OCEAN CURRENT COEXISTENCE ON THE WAVE AND CURRENT PREDICTIONS IN THE TSUGARU STRAIT

Ayumi Saruwatari[1], Yoshihiro Yoneko[2] and Yu Tajima[3]

The Tsugaru Strait between Hokkaido and Honshu islands, connecting the Pacific Ocean and Japan Sea, has been used for shipping and fishery. The current in the strait formed by a tidal current and ocean current so-called Tsugaru Warm Current is recently assumed to be one of the potential renewable energy source in Japan. The present study investigates the effects of the coexistence of the tidal/ocean currents as well as sea waves on the predictions of the physical conditions around this strait. We performed two different numerical experiments for characterising the physical environment associated with current-current and wave-current interactions. Harmonic analysis of the tidal current shows tidal ellipses of the diurnal and semi-diurnal constituents are stretched into the direction of the ocean current and enable to be reasonably predicted without considering the effect of the current-current interaction. Wave height in the strait is shown to vary 0.75–1.5 times of the original wave height by attenuated and amplified by the coexisting current. It will be indicated that the physical environment associated with the current-current and wave-current interactions should be considered for effective utilisation of this area.

INTRODUCTION

Tsugaru Strait locates between Hokkaido and Honshu islands of Japan, having the minimum width of 19 km and connecting the Pacific Ocean and Japan Sea. Current in the Tsugaru Strait is formed by tidal and ocean currents. Difference of the tidal range at the both sides of the strait causes tidal current. Eastward ocean current running from the Japan Sea to the Pacific Ocean, so-called the Tsugaru Warm Current, coexists with the tidal current, resulting that strong current more than 2 ms^{-1} can be formed at the two narrow necks of the strait. This area has been roundly used for fishery and shipping. Also, the current in this strait is assumed to be one of the potential renewable energy sources in Japan. Local government of Hakodate, facing to the strait, is planning a tidal energy project and has been conducted a field monitoring to investigate the energy resources in this area.

Several papers have reported that waves on a current can cause lower performance of a tidal stream turbine. Also co-existence of waves and a current causes amplification and attenuation of the waves. Disturbance from the waves as well as the wave deformation should be taken into account when we discuss performance of a energy device.

The present study investigates the effects of the coexistence of the tidal/ocean currents as well as sea waves on the predictions of the physical conditions around this strait. We performed two different numerical experiments: (1) Prediction of the current fields with/without considering the effects of the ocean current on the tidal current and (2) prediction of the wave fields with/without considering the effects of the current on the wave fields. Characterization of the physical environment associated with current-current and wave-current interaction will contribute effective utilization of this area.

COMPUTATION
Tidal and Ocean Currents

Current in the strait is represented as the sum of the tidal and ocean currents. Three dimensional velocity fields of the current were computed using MIT general circulation model (MITgcm) developed in Massachusetts Institute of Technology (Marshall et al., 1997ab). The model is known to solve three-dimensional non-hydrostatic Navier-Stokes equations for compressible fluid and can be applied to a flow with the order of 1 km to the global scale.

Figure 1 (*a*) shows the computational domain. The grid intervals are 30sec and 20sec into longitude and latitude direction, which are about 600 m around this location. The vertical grid intervals are 1–15 m that becomes finer into the water surface and coarser into the bottom. Computations were performed with the time step of 10 seconds during the period from 15th March 2013 00:00 to 21st April 2013 00:00 (UTC) which corresponds to the period Hakodate city conducted the field monitoring of the current at the location P1 (see Fig.1).

---

[1]Faculty of Engineering, Hokkaido University, Japan
[2]Hokkaido Electric Power Co. Inc., Japan
[3]Shueisha Inc., Japan
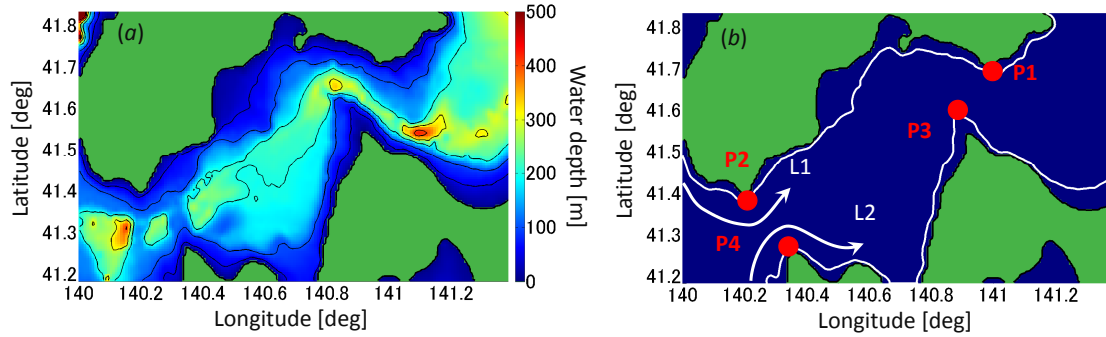
Figure 1: (*a*) **Computational domain for the MITgcm where the contour lines represent the water depth.** (*b*) **Definitions of the representative points P1–P4 and axes L1 and L2.**
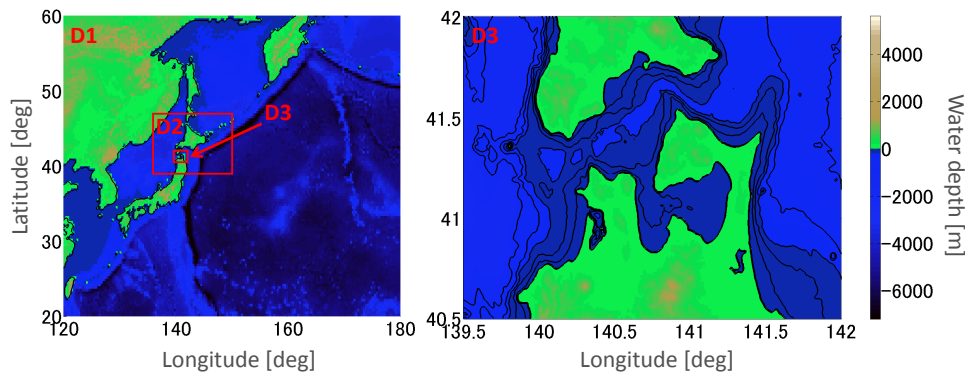
Figure 2: Computational domains for the wave computation.

Tidal and ocean current velocities were given as the boundary conditions. Tidal current velocity at the boundary was interpolated from a regional tidal solution of TPXO 7.2 around the Seas of Okhotsk and Japan with $1/30°$ resolution (Egbert and Erofeeva, 2002) for the eight major tidal constituents (M2, S2, N2, K2, K1, O1, P1, Q1). Reanalysis data FRA-JCOPE 2 (Japan Coastal Ocean Predictability Experiment, Miyazawa et al., 2009), with 5 minutes resolution provided every 24 hr by JAMSTEC (Japan Agency for Marine-Earth Science and Technology) were used for the input of the ocean current. Bathymetry data were obtained from GEBCO (General Bathymetric Chart of the Oceans) by BODC (British Oceanographic Data Centre) having 30 seconds resolution. Two cases of numerical experiments were performed: (case 1) only tidal current was given at the boundaries, (case 2) both tidal and ocean currents were given at the boundaries.
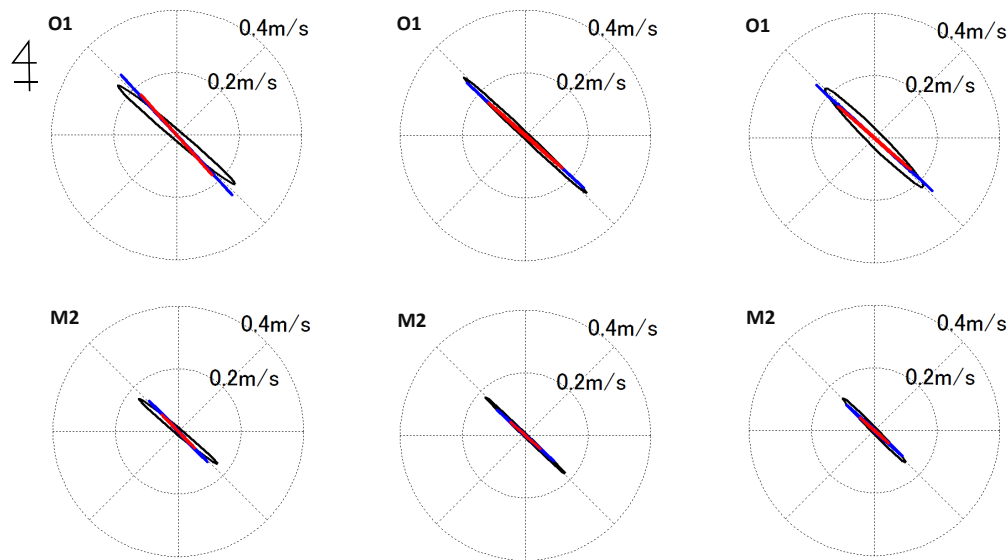
Figure 3: Comparison of tidal ellipses at P1 for the upper (left), middle (middle) and bottom (left) layers. Black: observation data by the field monitoring, Red: computational results in case 1, and Blue: computational results in case 2

Sea Waves

Wave energy fields were computed using a wave prediction model, Simulating Waves Nearshore (SWAN; Booij et al., 1999; Ris et al., 1999), developed at Delft University of Technology. The wave model solves action balance equations to obtain the distribution of the wave action density. The effects of a current coexisting with the waves are considered by changing the wave propagation velocity with the current velocity. The current velocity field obtained by the circulation model MITgcm as described earlier was input into the wave computation.

Three-domain nesting computations were performed with the grid resolutions of 20 minutes, 4 minutes and 30 seconds for the domains D1–D3, respectively (see Fig.2). Meteorological re-analysis data sets from ERA-Interim (45 minutes × 45 minutes resolution) provided by European Centre for Medium-Range Weather Forecasts (ECMWF) were used for the wind input for domain 1. Wind data with 6 minutes resolution, computed by using a meteorological model WRF (Weather Research and Forecasting) model, were input for domains 2–4 every hour. Computational period is 31 days from 1st October 2006 00:00 (UTC).

The present study conducted two more computations with the following computational cases too see characteristics of wave deformation in the strait: (case 3) wave field was calculated without the effects of the current, (case 4) wave field was calculated with the input of the tidal current.

RESULTS
Tidal Ellipses

Tidal ellipses at P1 were calculated to compare with that obtained from the field monitoring. Figure 3 shows the tidal ellipses in case 1–2 as well as the observed ones for diurnal (O1) and semidiurnal (M2) constituents. Tidal ellipses were shown for the upper, middle and bottom layers by dividing the water depth at P1 into 1/3 sections. Results from case 2 showed better agreement with that from the observations comparing to the results from case 1 that is underestimating the length of the major axes of the tidal ellipses. Distributions of the tidal ellipses for O1 and M2 tidal constituents near the point P1 in cases 1 and 2 are shown in Fig. 4 where the color represents the length of the semi-major axis of the ellipses. The ellipses are found to be stretched into the direction of the axis of the strait by the effect of the ocean current in case 2. The maximum velocity of the tidal current resulted in becoming larger by a coexisting ocean current, which
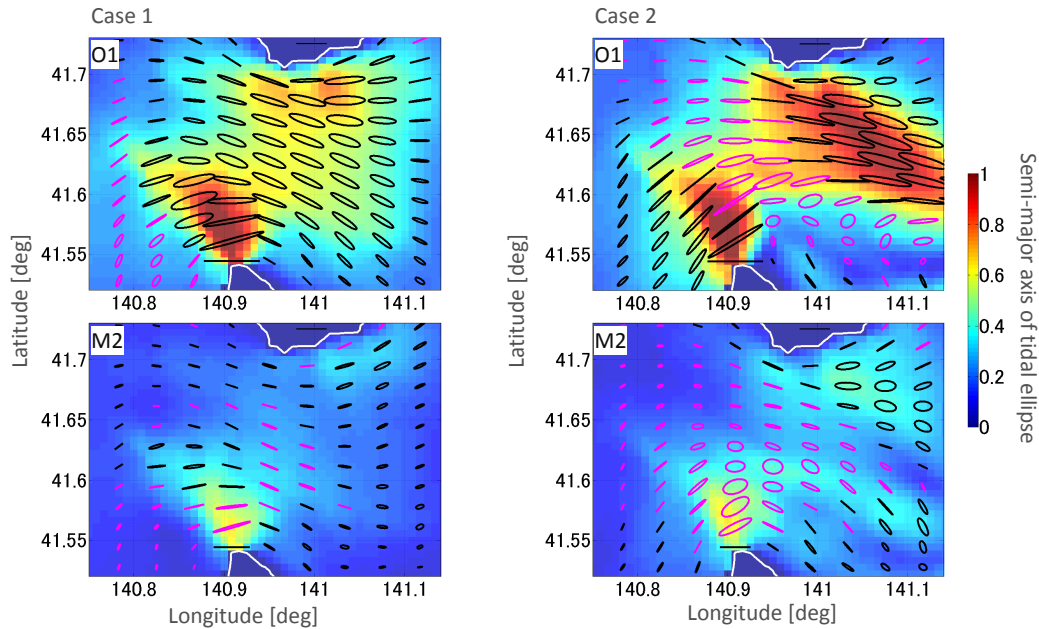
Figure 4: Distribution of tidal ellipses obtained in case 1 (left) and case 2 (right). Black and pink ellipses represent counter-clockwise and clockwise rotation, respectively. Diurnal constituent O1 (top) and semidiurnal constituent M2 (bottom).

explains the reason that the tidal ellipses in case 2 showed better agreement with the observed ones in Fig. 3. Consideration of the current-current interaction was found to be necessary for reasonable prediction of the tidal ellipses of this location. It is also possible that the coexistence of ocean and tidal currents increases the amount of the usable energy of the current in this strait since the maximum velocity of the each tidal constituent should become larger with the stretch of the tidal ellipses.

Ratio of the semi-major axis in case 2 to case 1 is shown in Fig. 5. It was found that the length of the semi-major axis near P1 can be around 1.25 times by the effect of the ocean current for the O1 tidal constituent, and can be more than 1.5 times for the M2 constituent.

Current Velocity Near the Coast Lines

In order to see the energy distribution of the tidal and ocean current near a coast line where is often selected as a site for power extraction from tidal and ocean currents, velocity distribution in the shallow water area was calculated based on the computed results in cases 2. Axes L1 and L2 were defined along the 50-m depth contour lines in the North and South sides of the strait (see Fig.1 (b)). Both axes are defined as positive into the East direction. Figure 6 represents the velocity distribution of the composite flow along L1 and L2 in case 2. The flow converges at the two necks of the strait to form strong currents. Points P2–P4 in addition to P1 were defined at the locations having the peak current velocities and indicated on Fig.1 (b). East neck of the strait was found to have a strong current in wider area rather than the West. The maximum velocity is expected to be around 2.0 ms^{-1} at P1, which is usable for power generation. Also at the other side of the strait, P3, 20% of the tidal velocity was found to become more than 2.0 ms^{-1}. Median velocity in the case computed with the effects of the ocean current (case 2) became 0.8–2.1 times larger than that without the ocean current (Case 1). This velocity difference corresponds to 0.3–9.3 times difference of the current energy that is proportional to the cube of the current velocity.

Wave Deformation Due to the Current

Wave amplification factor α was defined as a ratio of the significant wave height in case 4 (H) to that in case 3 (H_0) for measuring the wave deformation due to the coexisting current as proposed by Saruwatari
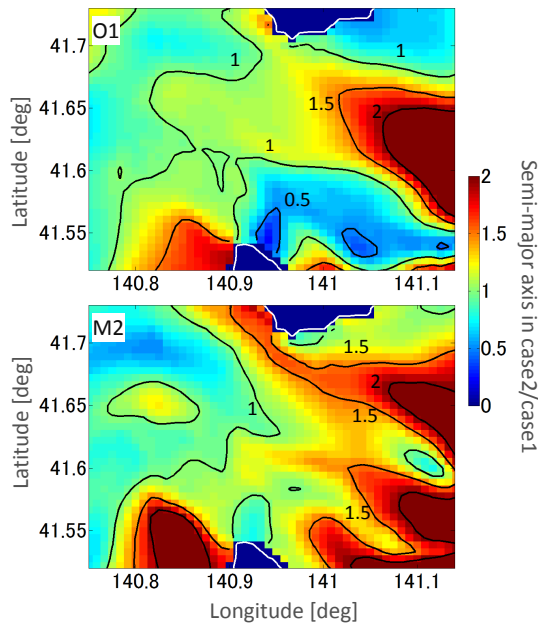
Figure 5: Distribution of the ratio of the semi-major axis in case 2 to case 1 around P1 in the strait. Diurnal constituent O1 (top) and semidiurnal constituent M2 (bottom).
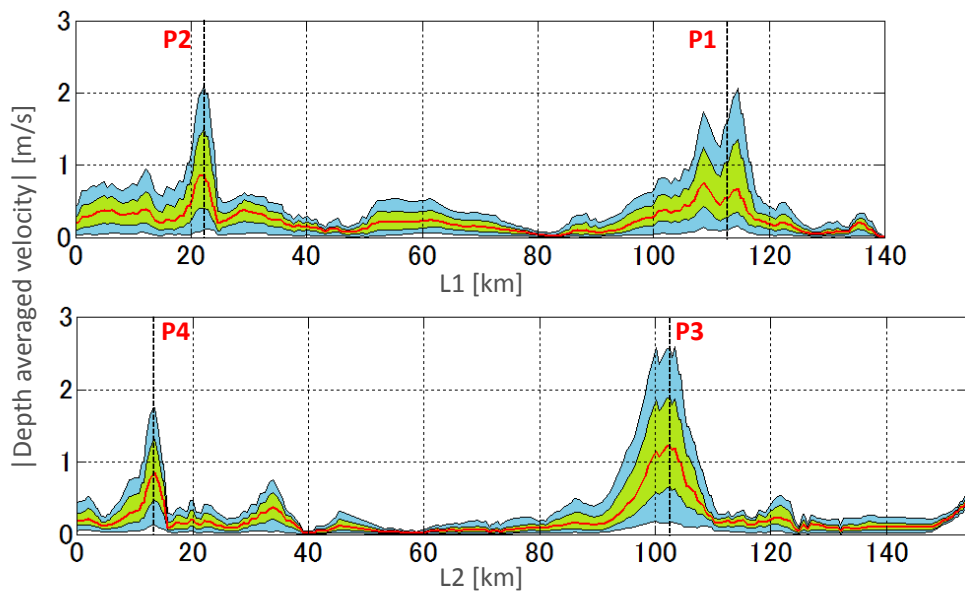
Figure 6: Velocity distribution along the axes L1 and L2 for the present computational period (case 2). Median current velocity (red), 25th to 75th percentile (green) and 5th to 95th percentile (blue) of the current velocity. P1–P4 are indicated in Fig.1.
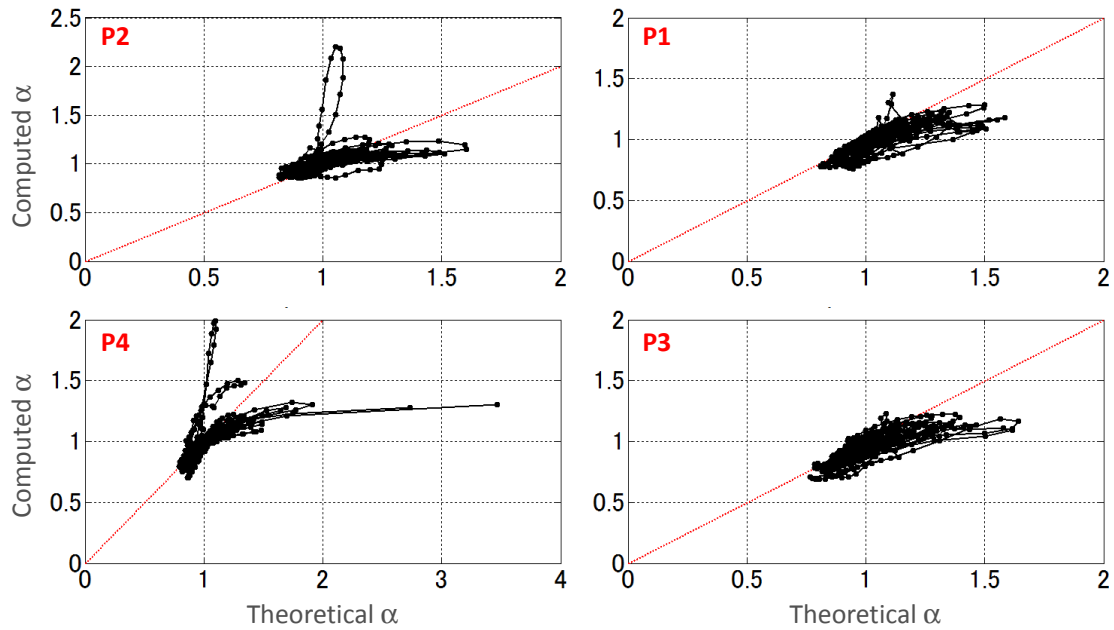
Figure 7: Comparison of the wave amplification factor obtained by the present computation with that predicted theoretically at P1–P4.

et al. (2013).

$$\alpha = H/H_0 \tag{1}$$

The amplification factor also can be theoretically obtained by the following equation when we assume small amplification waves on a steady current.

$$\alpha_T = \left[\left(1 + \frac{2k'h'}{\sinh 2k'h'} \right) \left(\frac{1}{k'} - U \right) + 2U' \right]^{-1/2} \tag{2}$$

Figure 7 is the comparison of the wave amplification factors computed in the present study and predicted theoretically at P1–P4. Theoretical amplification factor tended to overestimate the wave amplification when the current is flowing against the mean wave direction and the amplification factor is expected to be more than one, which is thought to be because the theoretical amplification factor does not account for wave breaking due to the amplification of the wave height. Large deviation of the computed amplification factor can be seen at P2 and P4 with the theoretical α being around one which therefore means the current velocity into the mean wave direction is almost zero. As the deviation was seen with a current flowing almost perpendicularly to the mean wave direction, it is thought that larger waves were propagated to this location by the coexisting current not by the wave amplification due to the current.

Relationship between the wave amplification factor and current velocity into the mean wave direction is shown in Fig. 8. The wave amplification factor was found to fluctuate between 0.75 and 1.5 at P1 and P3 with the effect of the tidal current of this strait. The fluctuation of the wave conditions would affect, for instance, the estimation of the wave force against marine energy devices installed in this area. We should therefore consider the effects of the current on the wave field.

CONCLUSION

We investigated general characteristics of the tidal and ocean current in the Tsugaru Strait especially near a location in which a tidal energy project is about to be proceeded. By conducting numerical experiments using a circulation model, tidal ellipses in the strait were found to be stretched into the direction of
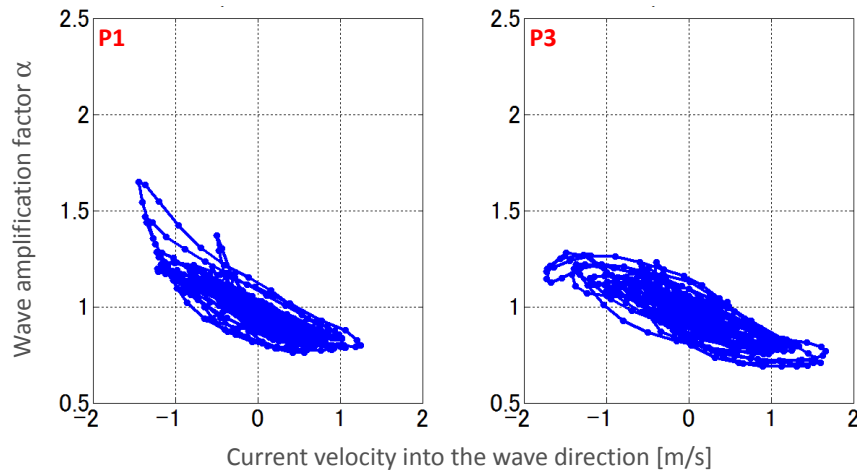
Figure 8: Relationship between the wave amplification factor and tidal current velocity into the mean wave direction at P1 (left) and P3 (right).

the ocean current, which means we have to consider the co-existence of both currents in order to reasonably evaluate the potential of the current energy. East side of the strait was found to have larger area to have sufficient current velocity for power generation than the west. Also by performing numerical experiments on wave amplification due to tidal currents in the strait, waves were found to be amplified 0.75 to 1.5 times of the original wave height, which means the wave deformation should be taken into account to estimate the effects of waves on the performance of a stream turbine.

REFERENCES
Marshall, J., A. Adcroft, C. Hill, L. Perelman and C. Heisey (1997a): A finite-volume, incompressible Navier Stokes model for studies of the ocean on parallel computers. *J. Geophys. Res.*, 102 (C3), pp. 5753–5766.

Marshall, J., C. Hill, L. Perelman and A. Adcroft (1997b): Hydrostatic, quasi-hydrostatic, and nonhydrostatic ocean modeling, *J. Geophys. Res.*, 102 (C3), pp. 5733–5752.

Miyazawa, Y., R. Zhang, X. Guo, H. Tamura, D. Ambe, J.-S. Lee, A. Okuno, H. Yoshinari, T. Setou and K. Komatsu (2009): Water mass variability in the western North Pacific detected in a 15-year eddy resolving ocean reanalysis, *J. Oceanogr.*, 65, pp. 737–756.

Egbert, G.D. and S.Y. Erofeeva (2002): Efficient Inverse Modeling of Barotropic Ocean Tides, *J. Atmos. Oceanic Technol.*, 19, 2, pp. 183–204.

Booij, N., R.C. Ris and L.H. Holthuijsen (1999): A third-generation wave model for coastal regions, Part I, Model description and validation, *J. Geophys. Res.*, 104 (C4), pp. 7649–7666.

Ris, R.C., N. Booij and L.H. Holthuijsen (1999): A third-generation wave model for coastal regions, Part II, Verification, *J. Geophys. Res.*, 104 (C4), pp. 7667–7681.

Saruwatari, A., D.M. Ingram and L. Cradden (2013): Wave-current interaction effects on marine energy converters, *Ocean Eng.*, 73, pp. 106–118.